Journal of Fluids and Structures (2002) **16**(7), 957–969
doi:10.1006/jfls.453 available online at http://www.idealibrary.com on IDEAL®

AEROACOUSTIC RESPONSE OF DIFFUSERS AND BENDS: COMPARISON OF EXPERIMENTS WITH QUASI-STEADY INCOMPRESSIBLE FLOW MODELS

S. DEQUAND, L. VAN LIER, A. HIRSCHBERG AND J. HUIJNEN

*Eindhoven University of Technology, Postbus 513, 5600 MB Eindhoven
The Netherlands*

(Received 18 April 2001; and in final form 15 February 2002)

Experimental results were obtained in the study of the aeroacoustic response of diffusers and abrupt expansions. An experimental study on the aeroacoustics of bends has also been carried out and shows similar results. In both cases, the low-frequency aeroacoustic behaviour can be predicted by a quasi-steady flow model when the flow separation point is fixed by sharp edges in the geometry. At smooth pipe discontinuities, nonlinear effects are more important and the response is essentially unsteady.

1. INTRODUCTION

BENDS AND CHANGES IN CROSS-SECTION (Figure 1) are typical pipe discontinuities encountered in gas-transport systems. Bends are inevitable to keep systems compact. Diffusers are used to reduce energy losses after a local increase of the flow velocity U_0 from about 20 m/s (Mach number of 0·05) up to 80 m/s (Mach number of 0·2). Such an increase of the flow velocity allows the use of smaller regulation valves or volume flow meters, which reduces considerably the costs of the system. Strong self-sustained oscillations of the flow can appear due to a coupling between vortex shedding at a closed side branch and acoustical standing waves in the pipe system (Bruggeman *et al.* 1989; Kriesels *et al.* 1995 Ziada & Shine 1999). As strong pulsations scale with $\rho_0 c_0 U_0$ (where ρ_0 is the density and c_0 is the speed of sound), an increase of the flow velocity U_0 by a factor of four implies an increase of amplitude of such pressure oscillations by at least a factor of four. Therefore, the prediction of such self-sustained oscillations becomes crucial. This prediction is difficult. When a bend is placed a few pipe diameters upstream of a closed side branch, it can strongly interfere with the pulsating closed side branch (Ziada & Shine 1999). This interaction vanishes for distances between the bend and the closed side branch of more than eight pipe diameters (Coffman & Berstein, 1979). It is expected from quasi-steady flow theory that the bend will then damp acoustical oscillations. One of the questions arising is, therefore, whether a quasi-steady flow theory can be used to describe the aeroacoustical response of bends. Such a theory is common in engineering practice to describe the response of a pipe system to imposed pulsations (Munjal 1987; Davis 1988).

For abrupt sharp-edged pipe expansions, extensive literature exists on the frequency dependence of the aeroacoustical response on low-amplitude pulsations (Ronneberger 1967, 1987; Cummings 1975; Åbom & Nilson 1995, Aurégan 1999). The linear response of a sharp-edged open pipe termination is also well understood (Rienstra 1981; Cargill 1982;

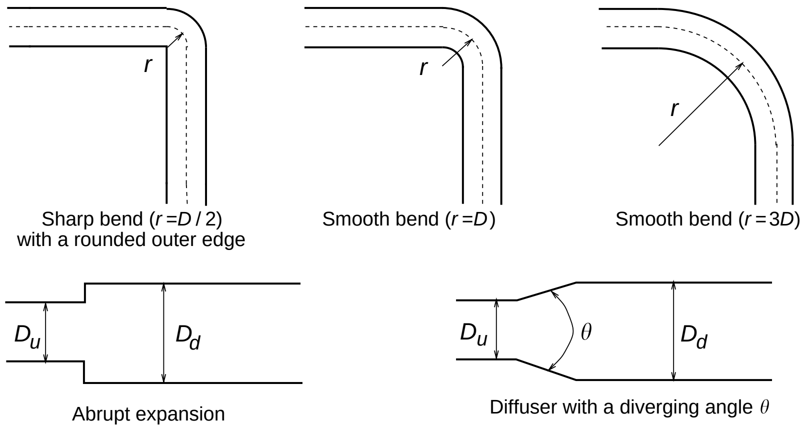

Figure 1. Configurations studied.

Munt 1990; Peters *et al.* 1993). Similar data are now available for thin sharp-edged orifices (Ingard & Ising 1967; Cummings 1983; Durrieu *et al.* 2001; Hofmans *et al.* 2001). Recently, Dequand *et al.* (2001) carried out a detailed study of the 90° bend with a sharp inner edge. Measured scattering matrices were compared with a quasi-steady flow theory and numerical flow simulations based on the Euler equations for inviscid and compressible flow. As for bends with a sharp inner edge, the sharp-edged abrupt expansions, the orifices and the open pipe terminations, the quasi-steady flow theory appeared to provide a reasonable prediction up to Strouhal numbers $\pi f D/U_0$, based on the pipe diameter D and the frequency f of the acoustical perturbations, of order unity. The aeroacoustical response of pipe discontinuities at which the flow separation point is not fixed by a sharp edge is much more complex and cannot easily be predicted numerically. Examples are the whistling behaviour of lip-shaped orifices (Wilson *et al.* 1971), thick diaphragms (Blake 1986) and rounded pipe terminations (Peters *et al.* 1993). Similar whistling behaviour was observed by van Lier *et al.* (2001) for a typical industrial diffuser placed at the junction of a pipe with a reservoir. His observations confirm the results of Kwong & Dowling (1994). This whistling phenomenon can be understood qualitatively in terms of the vortex sound theory of Howe (1998) and is similar to that of a whistler nozzle (Hill & Greene 1977; Hussain & Hasan 1983, Hirschberg *et al.* 1989). An interesting feature is that, in contrast to the behaviour of discontinuities with a flow separation point fixed by a sharp edge, the aeroacoustical behaviour of the diffuser is amplitude dependent (van Lier *et al.* 2001). At low amplitude, a spectacular whistling phenomenon is observed. It disappears for high acoustical particle velocities $|u'|$ compared to the main flow velocity U_0. When $|u'|/U_0$ is of order unity, the response of the diffusers is essentially quasi-stationary.

In the first part of this paper, we summarize the results obtained for a diffuser, stressing its essentially nonlinear behaviour. A more extensive discussion is provided by van Lier *et al.* (2001). We then consider the sound absorption by a 90° bend. We know that, in such subsonic isentropic flows, the aeroacoustical source responsible for this absorption has a dipole character and is associated with the modulation of the vortex shedding in the bend (Howe 1998). It is, therefore, obvious that the bend will be most effective in absorbing sound when it is placed at a pressure node in a standing wave within a pipe system. The simplest procedure to measure the sound absorption, due to the presence of a bend, is to compare the reflection coefficient of a pipe terminated by an open end without bend, with the reflection coefficient of the same pipe with a bend placed at a pressure node. Placing the bend close to the open pipe termination, within one or two pipe diameters, would not be representative for a bend in a long pipe. We, therefore, placed the bend a wavelength upstream of the open pipe termination. This, however, makes the experiment difficult to carry out with a variable frequency. We, therefore, worked at a fixed frequency and varied the flow velocity.

We limit our theoretical analysis to a quasi-steady incompressible flow theory. We present data for an abrupt pipe expansion and we compare them to data obtained for a diffuser with a diverging angle of 28°. We then compare the absorption of 90° bends with ratios $r/D = 0{\cdot}5$, 1 and 3, respectively (where r is the radius of curvature and D the pipe diameter).

2. EXPERIMENTAL METHOD

2.1. Description of the Experimental Set-up

The experimental method and set-up used are described in detail by Peters *et al.* (1993), Hofmans *et al.* (2001) and Durrieu *et al.* (2001). By means of the two-microphone method, the pressure reflection coefficient R_p is measured as a function of the Mach number $M = U_0/c_0$ for different pipe discontinuities (Fig 1). The Mach number is varied in the range $0 < M < 0{\cdot}3$ corresponding to Reynolds numbers $\mathrm{Re} = U_0 D/\nu$ up to 2×10^5, where ν is the kinematic viscosity of air and U_0 is the main flow velocity upstream of the discontinuity. A siren is used as a source of sound, which can modulate the flow periodically with an adjustable frequency f. The acoustical pressure is measured by means of piezoelectric microphones (type PCB 116A) coupled to charge amplifiers (Kistler type 5007). The signals are transferred to a data acquisition system (HP 3565S) which provides the transfer functions $H_{ij} = \hat{p}_i/\hat{p}_j$ between the signals of the two microphones at positions x_i and x_j. The pressure reflection coefficient is then determined from the transfer function H_{ij}, the position of the microphones x_i and x_j, and the wavenumbers k^+ and k^-:

$$k^{\pm} = \frac{1}{1 \pm M}\left(\frac{2\pi f}{c_0} - \mathrm{i}\alpha_0 Z\right), \tag{1}$$

where α_0 is the damping without mean flow (Kirchhoff) and Z is the wall impedance as measured by Ronneberger (1977) and Peters *et al.* (1993). We used a fit of the Peters *et al.* data for Z as proposed by Hofmans *et al.* (2001).

In the following two sections, the geometry of the configurations studied is described more accurately. In all experiments, the pipes have a circular cross-section and the wall thickness is 5 mm. The pipes are smooth within $0{\cdot}1\,\mu$m. The bends and diffusers have a wall roughness of $<0{\cdot}01$ mm.

2.1.1. Diffusers

In the experimental study of the diffusers, the frequency $f = 289$ Hz is used. The ratio of the downstream cross-section S_d to the upstream cross-section S_u of the diffusers is $S_d/S_u = 25/9$ (the pipe diameters downstream and upstream are respectively $D_d = 4{\cdot}99$ and $D_u = 3{\cdot}00$ cm). Measurements have been carried out on an abrupt expansion and on a diffuser with a diverging angle $\theta = 28°$. This value corresponds to a typical diverging angle of industrial diffusers. The reflection coefficient was measured just upstream of the diffuser at $x = 0$ (Figure 2). The positions of the pressure transducers were: $x_1 = -0{\cdot}1097$ m, $x_2 = -0{\cdot}2135$ m, $x_3 = -0{\cdot}4107$ m, $x_4 = -0{\cdot}5084$ m and $x_5 = -0{\cdot}6977$ m.

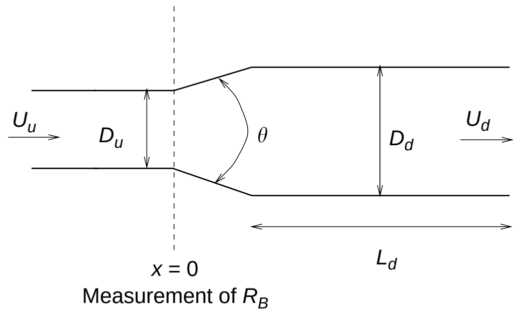

Figure 2. Geometry of the diffusers ($U_u = U_0$).

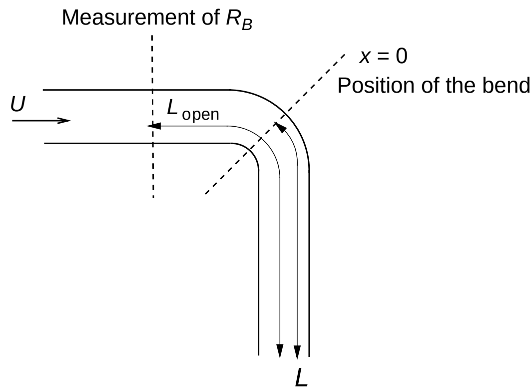

Figure 3. Geometry of the bends.

The diffuser was placed upstream of a pipe segment of length $L_d = 1{\cdot}2\,\text{m}$ which corresponds to one wavelength. In order to be allowed to use a fit of the experimental data of Peters *et al.* (1993) and to use the theory of Cargill (1982), special care was taken to have a sharp-edged open pipe termination.

2.1.2. Bends

In the experimental study of the bends, the pipe diameter was $D = 3\,\text{cm}$. The frequency oscillations of the source was fixed to $f = 343\,\text{Hz}$, except for the bend with centre-line radius $r = 3D$ where the frequency was fixed to $f = 344{\cdot}5\,\text{Hz}$. The reflection coefficient was measured at $L_{\text{open}} = 1{\cdot}001\,\text{m}$ from the open pipe termination. The position of the bends ($x = 0$) relatively to the open pipe termination was different for each bend (Figure 3): (i) for the bend $r = D/2$: $L = 0{\cdot}519\,\text{m}$; (ii) for the bend $r = D$: $L = 0{\cdot}505\,\text{m}$, (iii) for the bend $r = 3D$: $L = 0{\cdot}441\,\text{m}$.

The relative positions of the pressure transducers were: $x_2 - x_1 = -0{\cdot}1895\,\text{m}$, $x_3 - x_1 = -0{\cdot}2870\,\text{m}$, $x_4 - x_1 = -0{\cdot}4843\,\text{m}$ and $x_5 - x_1 = -0{\cdot}5880\,\text{m}$.

2.2. Determination of the Reflection Coefficient

Our experiments were carried out in the presence of a mean flow. Therefore, we present our experimental results for the reflection coefficient R_B of the acoustic enthalpy:

$$|R_B| = |R_p|\frac{1-M}{1+M}, \tag{2}$$

rather than the pressure reflection coefficient R_p. The advantage of using the enthalpy reflection coefficient R_B is that it provides a direct measure of the energy absorption which is the most interesting information for designing pipe systems.

The reflection coefficient at the open pipe termination is calculated from

$$R_{\text{end}} = -(1+\mathscr{A}M)\left(1-\frac{1}{2}\left(\frac{\pi f D}{c_0}\right)^2\right)\mathrm{e}^{\mathrm{i}\Phi}, \tag{3}$$

where $\mathscr{A}$ is a fit of the theory of Cargill (1982) proposed by Hofmans *et al.* (2001):

$$\mathscr{A}(Sr) = \begin{cases} \mathrm{Sr}^2/3 & \text{for } 0 \leq \mathrm{Sr} < 1 \\ (2\mathrm{Sr}-1)/3 & \text{for} 1 \leq \mathrm{Sr} < 1{\cdot}85, \\ 0{\cdot}9 & \text{for } 1{\cdot}85 \leq Sr \end{cases} \tag{4}$$

with $\mathrm{Sr} = \pi f D/U$ the Strouhal number, D the pipe diameter and U the main flow velocity ($D = D_d$ and $U = U_d$ for the diffuser). The phase Φ of the reflection coefficient at the pipe termination [equation (3)] is determined from the end corrections δ_{end} measured by Peters *et al.* (1993):

$$\Phi = -2k\delta_{\text{end}}, \tag{5}$$

with $\delta_{\text{end}} \approx 0{\cdot}31D$ and k the wave number.

The reflection coefficient was determined at a fixed position $x = 0$ from the open pipe termination. This reduces differences due to damping during wave propagation along the pipe between the reference straight pipe and the pipe with bend. As the losses are determined by the difference between R_B measured with and without bend, we automatically compensate for the acoustics of the room. This, however, is not perfect because the position of the pipe termination is moved within the room by introducing the bend. Because we displace by a distance of a wavelength in a direction parallel to the walls of the room, this effect will be very small for most room modes. Furthermore, our laboratory was very large, so that the confinement effects were limited. Detailed information is provided by Peters *et al.* (1993).

3. PREDICTION OF THE REFLECTION COEFFICIENT

3.1. Scattering Matrix Representation

The scattering matrix representation is a common way to describe discontinuities in ducts. Below the cut-off frequency f_c, the solution of the wave equation can be written as a d'Alembert solution, that is to say a superposition of two plane waves: one travelling wave in the positive x-direction and another in the negative x-direction. Figure 4 shows the representation of plane waves in a duct where the discontinuity is replaced by an acoustic two-port at the position $x = 0$.

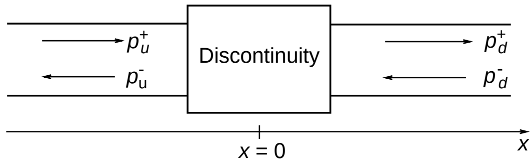

Figure 4. Plane waves decomposition in a duct.

In the scattering matrix representation, the wave upstream of the discontinuity is decomposed into two waves: an incoming wave p_u^+ and an outgoing wave p_u^-. The same decomposition is made downstream of the discontinuity. The scattering matrix $\mathcal{S}$ relates the outgoing plane waves p_u^- and p_d^+ to the incoming plane waves p_u^+ and p_d^-:

$$\begin{Bmatrix} p_d^+ \\ p_u^- \end{Bmatrix} = \underbrace{\begin{bmatrix} T_p^+ & R_p^- \\ R_p^+ & T_p^- \end{bmatrix}}_{\mathcal{S}} \begin{Bmatrix} p_u^+ \\ p_d^- \end{Bmatrix} = \frac{1}{2 + MC_d} \begin{bmatrix} 2 & MC_d \\ MC_d & 2 \end{bmatrix} \begin{Bmatrix} p_u^+ \\ p_d^- \end{Bmatrix}, \qquad (6)$$

where C_d is the loss coefficient discussed further in Section 3.2.2. The components R_p^+ and T_p^+ of the scattering matrix represent, respectively, the reflection and transmission coefficients of the incoming wave p_u^+ when the downstream termination is anechoic ($p_d^- = 0$). R_p^- and T_p^- have a similar interpretation.

3.2. Quasi-Steady Flow Theories

3.2.1. Bends: incompressible quasi-steady flow theory

At low Strouhal numbers $\pi fD/U_0 \ll 1$, we can predict the scattering matrix defined in the previous section by means of a quasi-steady flow model as developed by Durrieu *et al.* (2001) and Hofmans *et al.* (2001) for the orifice. We compare our experimental data obtained for the bends at Strouhal numbers in the range $0{\cdot}3 < \pi fD/U_0 < 3$ with an incompressible quasi-steady flow theory. In the incompressible flow model, three equations are written: the mass conservation law, the Bernoulli equation in the jet and the momentum conservation law across the turbulent mixing region downstream of the jet. Different assumptions are made: (i) only plane waves propagate far away from the discontinuity; (ii) compact source region; (iii) flow separation at the discontinuity and jet formation (*vena contracta* effect); (iv) incompressible and irrotational flow in the jet; (v) no wall friction in the turbulent mixing region after the jet (Figure 5).

The sharp bend ($r = D/2$) is better described by a compressible quasi-steady flow theory. However, the difference between the incompressible and the compressible flow theories becomes significant only at high Mach numbers (typically $U_0/c_0 > 0{\cdot}1$).

In the case of smooth bends ($r = D$ and $3D$), it is not obvious anymore to assume a free jet formation with a *vena contracta* effect at the pipe discontinuity. The experimental data obtained for the smooth bends could be compared to a Fanno model. Modelling the smooth bend $r = 3D$ as a straight pipe with a finite friction region would intuitively be more adapted (Figure 6).

A *vena contracta* ratio is, however, deduced from the values of the loss coefficient C_d reported by Blevins (1984) for different bend curvatures, and the experimental data are compared to an incompressible quasi-steady flow theory.

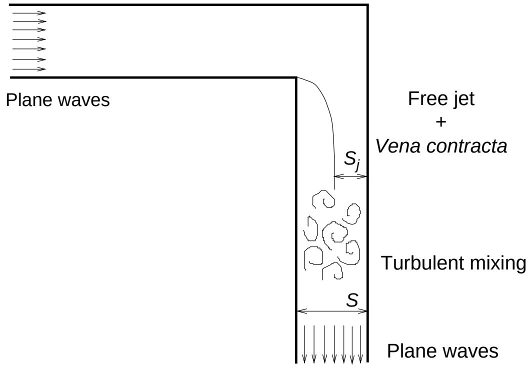

Figure 5. Quasi-steady behaviour of the flow in a sharp bend.

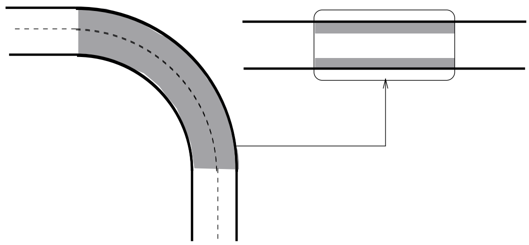

Figure 6. The smooth bend as a straight pipe with a finite friction region.

3.2.2. Loss coefficient

The loss coefficient C_d is defined as the ratio between the pressure difference $\Delta p = p_u - p_d$ and the upstream dynamic pressure:

$$C_d = \frac{p_u - p_d}{\frac{1}{2}\rho_0 U_0^2}. \tag{7}$$

The value of the loss coefficient C_d gives an estimation of the *vena contracta* effect which is a contraction of the jet occurring after the flow separation. C_d depends on the geometry of the discontinuity and on the Reynolds number $U_0 D/v$ (where U_0 is the main flow velocity, D a typical length of the system, and v the kinematic viscosity).

For the bends, at small r/D, losses increase because of separation. At larger r/D, losses increase due to increasing length of the bend. Following Blevins (1984), because our Reynolds numbers are typically between 10^4 and 10^5, we chose $C_d = 0{\cdot}4$ and $0{\cdot}25$ for the bends $r = D$ and $3D$, respectively. For the sharp bend ($r = D/2$), the *vena contracta* ratio was calculated by means of a method based on potential flow theory. We found $S_j/S = 0{\cdot}5255$ which corresponds to a loss coefficient $C_d = (S/S_j - 1)^2 = 0{\cdot}8153$ (with S_j the jet cross-section and S the pipe cross-section) (Dequand *et al*. 2001).

3.2.3. Diffusers: two quasi-steady flow limiting cases

In the case of diffusers, the aeroacoustic behaviour will depend on the amplitude of the acoustical velocity relatively to the main flow velocity $|u'|/U_0$. For weak perturbations, the behaviour of the diffuser will be compared to the steady state behaviour without flow

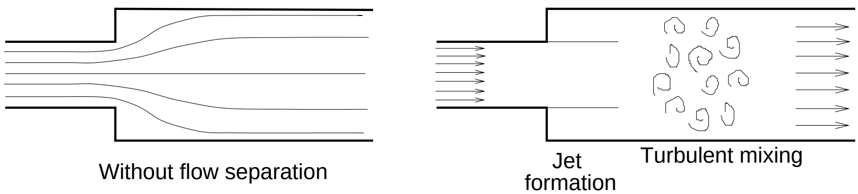

Figure 7. Two quasi-steady flow limiting cases in a diffuser.

separation. For strong pulsations, the behaviour will alternate between two quasi-steady flow limiting cases each half of the oscillation period: one quasi-steady flow model without flow separation, and one quasi-steady flow model with flow separation (Figure 7).

When the acoustic acceleration is in the same direction as the mean flow, the acoustic pressure gradient counteracts the stationary adverse pressure gradient and the separation point moves downstream. When the perturbation is strong enough, the separation point can disappear completely. Half an oscillation period later, the acoustic acceleration changes sign. The separation point is moving upstream and for strong enough perturbations, the separation will start at the diffuser inlet (the flow separation will be complete). If we assume that the acoustical perturbations are harmonic, then the behaviour of the diffusers is expected to be the geometrical mean of the two quasi-steady flow models (with and without flow separation).

In the quasi-steady flow theory without flow separation, three equations are written: (i) the mass conservation, (ii) the Bernoulli equation, (iii) the isentropic gas relation.

In the quasi-steady flow theory *with* flow separation, we write again the two first equations, but the isentropic gas relation is not valid anymore because there is an entropy generation due to the dissipation in the turbulent mixing region (Ronneberger 1967). The third equation is obtained by writing the momentum conservation law applied to the turbulent region.

4. RESULTS

4.1. Aeroacoustic Behaviour of Diffusers

4.1.1. Abrupt expansion placed in a long pipe

In the case of an abrupt expansion in the presence of a mean flow, a jet is formed at the junction between the upstream and the downstream pipe. When the abrupt expansion is placed in a long pipe, the jet flow becomes unstable and a turbulent mixing region appears. After a distance of several pipe diameters D_d, the flow becomes stable again. This phenomenon can be described by the quasi-steady flow theory with flow separation (Ronneberger 1967) explained roughly in the previous section. The study of such a configuration was an interesting test-case for the quasi-steady flow theory.

Figure 8 presents the Mach number dependence of the reflection coefficient $|R_B|$ for the enthalpy. The measurements have been carried out with a downstream pipe of a length close to one wavelength and at a fixed frequency $f = 289$ Hz (Section 2). The prediction of the reflection coefficient by the quasi-steady flow theory is good even for high Strouhal numbers $\pi f D/U_0 = \mathcal{O}(1)$ while the model is expected to be valid only for low Strouhal numbers $\pi f D/U_0 \ll 1$. We can notice the influence of the room acoustics on the reflection

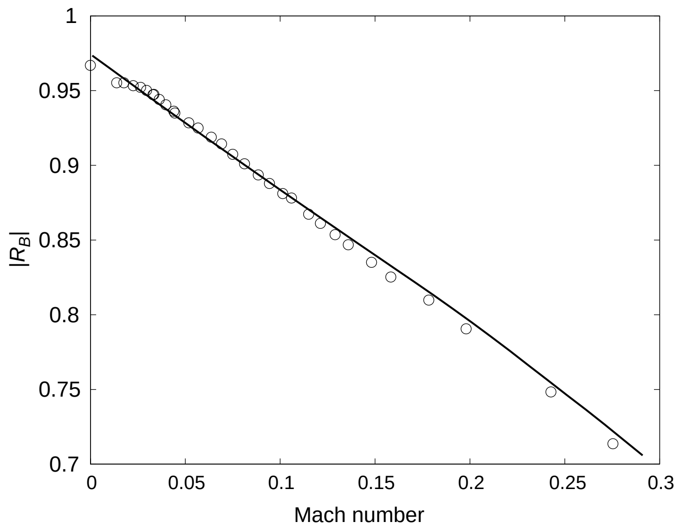

Figure 8. Enthalpy reflection coefficient $|R_B|$ in terms of the upstream Mach number U_0/c_0 for an abrupt expansion with $S_d/S_u = 25/9$, $L_d = 1{\cdot}2558\,\mathrm{m}$, $f = 289\,\mathrm{Hz}$. The solid line is the solution of the quasi-steady flow model with flow separation.

coefficient by comparing the limit $U_0/c_0 \to 0$ of the model with the measurements without mean flow.

4.1.2. Diffuser placed in a long pipe

In the case of a diffuser, nonlinear effects are important. The behaviour of the diffuser will depend on the amplitude of the acoustic perturbations. The separation point is not fixed as in an abrupt expansion but may move along the diverging walls of the diffuser. The measurements were made on a 28° diffuser placed in a long pipe ($L_d = 1{\cdot}2\,\mathrm{m}$) for three different perturbation amplitudes: $|u'|/U_0 \approx 0{\cdot}1$, $0{\cdot}4$ and 1. The results show quite a spectacular behaviours for the diffuser (Figure 9).

At relatively low perturbation amplitudes ($|u'|/U_0 \approx 0{\cdot}1$ and $0{\cdot}4$), oscillations of the reflection coefficient are observed and indicate either a sound production or a sound absorption depending on the Strouhal number. The behaviour is essentially nonlinear and is not predicted by the quasi-steady flow model. At Mach number $U_0/c_0 = 0{\cdot}13$, the maximum of the sound production is the most distinct. The fact that R_B is larger than the theoretical value without flow separation confirms sound production. In the case of a diffuser placed close to the open pipe termination, R_B can even become larger than unity. This indicates that the system can induce self-sustained oscillations (van Lier *et al.* 2001). The influence of the perturbation amplitudes is quite obvious when we compare the maxima of the oscillations for $|u'|/U_0 \approx 0{\cdot}1$ and $0{\cdot}4$. The decrease in the sound production with increasing amplitudes appears because of a saturation of the sound source due to the discrete vortex formation (van Lier *et al.* 2001). When the perturbation amplitude is decreasing further than $|u'|/U_0 \approx 0{\cdot}1$, the sound production becomes again independent of the amplitude.

At higher pulsation amplitudes ($|u'|/U_0 = \mathcal{O}(1)$), the diffuser shows a different behaviour. The diffuser becomes a strong absorber. For low Mach numbers $U_0/c_0 \leq 0{\cdot}04$, the reflection coefficient $|R_B|$ is well predicted by the quasi-steady flow model with flow separation over half an oscillation period (Section 3.2.3). For higher

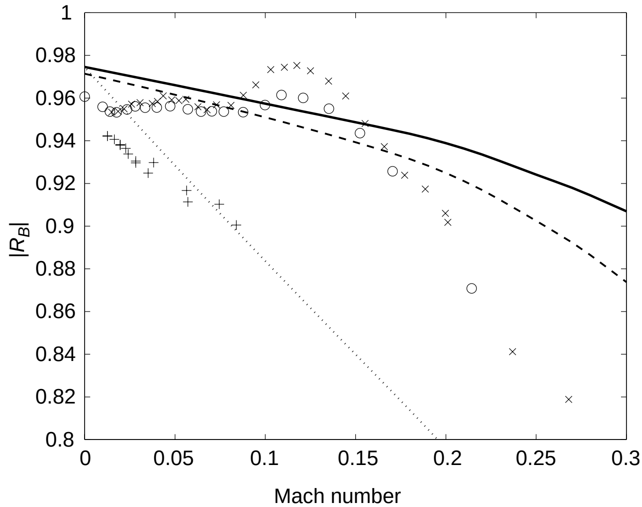

Figure 9. Enthalpy reflection coefficient $|R_B|$ in terms of the Mach number U_0/c_0 for a 28° diffuser with $S_d/S_u = 25/9$. Influence of the amplitude of the acoustical perturbation: $\times, |u'|/U_0 \approx 0{\cdot}1$; o, $|u'|/U_0 \approx 0{\cdot}4$; $+, |u'|/U_0 \approx 1$; —, quasi-steady flow model without flow separation; ....., high amplitude quasi-steady compressible flow model (with flow separation); - - - analytical low Mach number theory.

Mach numbers, the behaviour of the diffuser can be predicted by an intermediate case between the quasi-steady flow theory with flow separation and the quasi-steady flow theory without flow separation.

4.2. Aeroacoustic Behaviour of Bends

4.2.1. Sharp bend

The experimental data obtained for the sharp bend ($r = D/2$) are compared to an incompressible quasi-steady flow theory. The results are presented for the reflection coefficient $|R_B|$ for the total enthalpy in terms of the Mach number U_0/c_0.

In Figure 10, experimental and theoretical results for a straight pipe of the same length as the bend are also shown. It is quite obvious that the quasi-steady flow model gives a fair prediction of the aeroacoustic behaviour of the sharp bend. The influence of the presence of a sharp bend in a pipe is important.

4.2.2. Smooth bends

In the case of smooth bends, the prediction of the reflection coefficient by means of a quasi-steady flow theory is not reliable anymore. In such a case, it seems better to assume that the bends behave as a straight pipe segment.

Figure 11 shows the reflection coefficients of the smooth bends $r = D$ and $3D$, and for a straight pipe of the same length ($L = 1{\cdot}001$ m) in terms of the Mach number. The incompressible quasi-steady flow theory is applied to each bend. As mentioned earlier, it is not obvious that a free jet is formed in the case of smooth bends. The aeroacoustic behaviour of a smooth bend might depend on the amplitude of the acoustical perturbations as in the case of a diffuser. However, the influence of the acoustical perturbation amplitude has not yet been systematically studied.

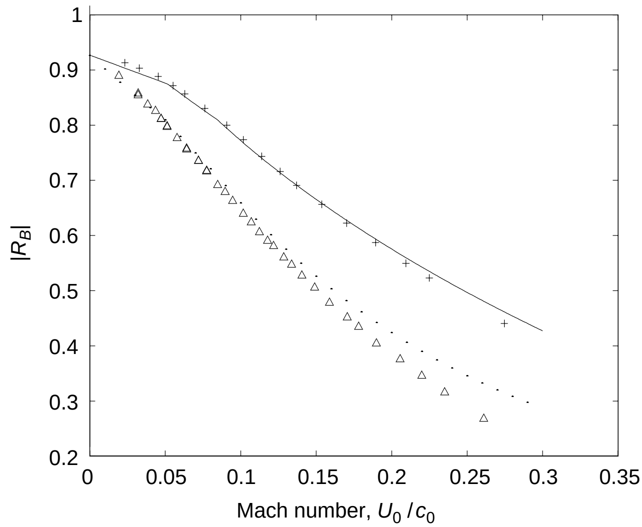

Figure 10. Enthalpy reflection coefficient $|R_B|$ in terms of the Mach number U_0/c_0 for a sharp bend ($r = D/2$): $\triangle$ experimental data; ....., incompressible quasi-steady flow theory; $+$, —, experimental and theoretical data for a straight pipe.

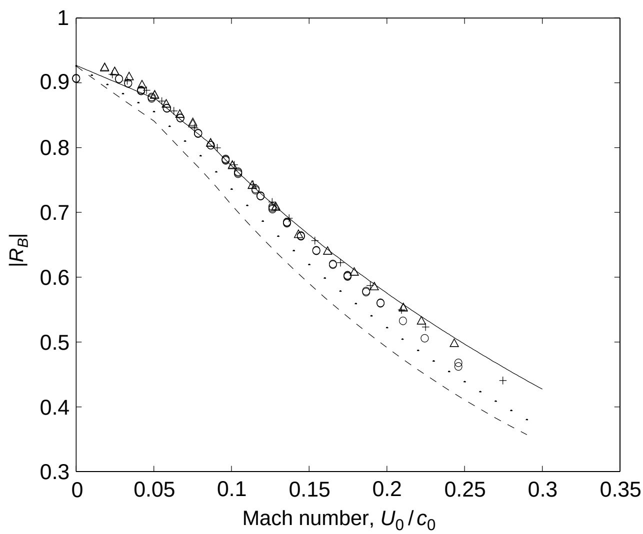

Figure 11. Enthalpy reflection coefficient $|R_B|$ in terms of the Mach number U_0/c_0 for smooth bends such as $r = D$ ($\triangle$) and $3D$ (o); incompressible quasi-steady flow theories for $r = D$ (.....) and for $r = 3D$ (- - -) ; experimental and theoretical data for a straight pipe (+ and —).

The results show that it is better to assume that there is no bend at all, rather than predict the behaviour of smooth bends by means of a quasi-steady flow theory based on measured values of C_d. The observed difference between the behaviour of a $r = D$ bend and a straight pipe is negligible, while the quasi-steady flow theory does predict a significant difference. For a $r = 3D$ bend, we observe only about 30% of the predicted difference.

It is noticed that the theory does not converge towards the experimental results at the limit $U_0/c_0 \to 0$. This is due to the influence of room acoustics as in the case of the experiments with the diffuser.

5. CONCLUSION

A parallel can be made between the aeroacoustic behaviour of bends and diffusers. In the cases of an abrupt expansion and a sharp bend ($r = D/2$), a jet is formed after the flow separation at the sharp edge. This behaviour is well predicted by an incompressible quasi-steady flow model up to Mach numbers U_0/c_0 of the order of 0·3 and for Strouhal numbers $\pi f D/U_0$ less than three.

In the case of a diffuser, the aeroacoustic response depends strongly on the amplitude of the acoustical perturbations. For relatively low perturbation amplitudes $|u'|/U_0 = \mathcal{O}(10^{-1})$, the behaviour is essentially nonlinear and is not predicted by the quasi-steady flow model. For high perturbation amplitudes $|u'|/U_0 = \mathcal{O}(1)$, the aero-acoustic response can be predicted by a quasi-steady flow model, alternating each half of an oscillation period between a model with flow separation and a model without. The study of the aeroacoustic response of smooth bends shows a quite similar behaviour. The reflection coefficient of a smooth bend is not predicted by an incompressible quasi-steady flow theory. It seems better in such a case to assume that there is no bend at all, rather than to use a quasi-steady flow model. As for the diffuser, the behaviour of a smooth bend is nonlinear. It would be interesting to study the influence of the amplitude of the acoustic perturbations on the aeroacoustic response. This has not yet been studied.

ACKNOWLEDGEMENTS

This work has been carried out within the framework of the European Project ‘Flow Duct Acoustics’ (FLODAC, BRPR CT97-10394) and with the support of Gasunie N. V. (Dr. H. Riezebos).

References

Åbom, M. & Nilson, B. 1995 Sound transmission at a sudden area expansion in a flow duct. *Proceedings of the 15th International Congress on Acoustics, Trondheim, Norway*, 563–566.

Aurègan, Y. 1999 Comportement aéro-acoustique basses fréquences d'une expansion. *14e Congrès Francais de Mécanique*, no. 451 on CDRom, Toulouse, France.

Blake, W. K. 1986 *Mechanics of Flow-Induced Sound and Vibration. Vol. 1: General Concepts and Elementary Sources*. Academic Press: Orlando.

Blevins, R. D. 1984 *Applied Fluid Dynamics Handbook*. New York: Van Nostrand Reinhold Company.

Bruggeman, J. C., Hirschberg, A., van Dongen, M. E. H., Wijnands, A. P. J. & Gorter, J. 1989 Flow induced pulsations in gas-transport systems: analysis of the influence of closed side branches. *ASME Journal of Fluids Engineering* **111**, 484–491.

Cargill, A. M. 1982 Low frequency acoustic radiation from a jet pipe—a second order theory. *Journal of Sound and Vibration* **83**, 339–354.

Coffman, J. T. & Berstein M. D. 1980 Failure of safety valves due to flow induced vibration. *ASME Journal of Pressure Vessel Technology* **102**, 112–118.

Cummings, A. 1975 Sound transmission at sudden area expansions in circular ducts, with superimposed mean flow. *Journal of Sound and Vibration* **91**, 503–518.

Cummings, A. 1983 High amplitude acoustic transmission through duct terminations: theory. *Journal of Sound and Vibration* **35**, 451–477.

DAVIS, P. O. A. L. 1988 Practical flow duct acoustics. *Journal of Sound and Vibration* **72**, 91–115.

DEQUAND, S., HULSHOFF, S. J., AURÉGAN, Y., HUIJNEN, J., VAN LIER, L. J. & HIRSCHBERG, A. 2001 Acoustics of 90 degree sharp bends. Part II: Low-frequency aeroacoustical response. Submitted to Acta Acustica.

DURRIEU, P., HOFMANS, G., AJELLO, G., BOOT, R., AURÉGAN, Y., HIRSCHBERG, A. and PETERS, M. C. A. M. 2001 Quasi-steady aero-acoustic response of orifices. *Journal of the Acoustical Society of America* **110**, 1859–1872.

HILL, W. G. & GREENE, P. R. 1977 Increased turbulent jet mixing rates obtained by self-excited acoustic oscillations. *ASME Journal of Fluids Engineering* **99**, 520–525.

HIRSCHBERG, A., BRUGGEMAN, J. C., WIJNANDS, A. P. J. & SMITS, N. 1989 The whistler nozzle and horn as aeroacoustic sound sources in pipe systems. *Acustica* **68**, 157–160.

HOFMANS, G. C. J., BOOT, R. J. J., DURRIEU, P. P. J. M., AURÉGAN, Y. & HIRSCHBERG, A. 2001 Aeroacoustic response of a slit-shaped diaphragm in a pipe at low Helmholtz number. Part I: Quasi-steady results. *Journal of Sound and Vibration* **244**, 35–56.

HOWE M. S. 1998 *Acoustics of Fluid-Structure Interactions*. Cambridge: Cambridge University Press.

HUSSAIN A. K. M. F. & HASAN M. A. 1983 The whistler nozzle phenomenon. *Journal of Fluid Mechanics* **134**, 431–458.

INGARD, K. U. & ISING, H. 1967 Acoustic non-linearity of an orifice. *Journal of the Acoustical Society of America* **42**, 6–17.

KRIESELS, P. C., PETERS, M. C. A. M., HIRSCHBERG, A., WIJNANDS, A. P. J., IAFRATI, A., RICCARDI, G., PIVA, R. & BRUGGEMAN, J. C. 1995 High-amplitude vortex-induced pulsations in a gas-transport system. *Journal of Sound and Vibration* **184**, 343–368.

KWONG, A. H. M. & DOWLING, A. P. 1994 Unsteady flow in diffusers. *ASME Journal of Fluids Engineering* **116**, 842.

VAN LIER, L., DEQUAND, S., HIRSCHBERG, A. & GORTER, J. 2001 Aeroacoustics of diffusers: an experimental study of typical industrial diffusers at Reynolds numbers of $O(10^5)$. *Journal of the Acoustical Society of America* **109**, 108–115.

MUNJAL, M. L. 1987 *Acoustics of Ducts and Mufflers: with Applications to Exhaust and Ventilation System Design*. Chichester: Wiley-Interscience.

MUNT, R. M. 1990 Acoustic transmission properties of a jet pipe with subsonic jet flow I. the cold jet reflection coefficient. *Journal of Sound and Vibration* **142**, 413–436.

PETERS, M. C. A. M., HIRSCHBERG, A., REIJNEN, A. J. & WIJNANDS, A. P. J. 1993 Damping and reflection coefficient measurements for an pipe at low Mach and low Helmholtz numbers. *Journal of Fluids and Mechanics* **256**, 499–534.

RIENSTRA, S. W. 1981 On the acoustical implications of vortex shedding from an exhaust pipe. *ASME, Journal of Engineering for Industry* **103**, 378–384.

RONNEBERGER, D. 1967 Experimentelle Untersuchungen zum akustischen Reflektionfaktor von unstetigen Querschnittsänderungen in einem luftdurchströmten Rohr. *Acustica* **19**, 222–235.

RONNEBERGER, D. 1987 Theoretische und experimentelle Untersuchungen der Schallausbreitung durch Querschnittsprunge und Lochplattent in Strömunggskanalen. Technical Report, Drittes Physikalisches Institut der Universität Göttingen.

WILSON, T. A., BEAVERS, G. S., DE COSTER, M. A., HOLGER, D. K. & REGENFUSS, D. 1971 Experiments on the fluid mechanics of whistling. *Journal of the Acoustical Society of America* **50**, 366–372.

ZIADA, S. & SHINE, S. 1999 Strouhal numbers of flow excited resonance of closed side-branches. *Journal of Fluids and Structures* **13**, 127–142.